# Development and implementation of a robot structure with adaptive stiffness by combining particle and layer jamming

Linda Weisheit
*Department Functionalization Technologies*
*Fraunhofer Institute for Machine Tools and Forming Technology*
Dresden, Germany
0000-0002-0403-6233

Lukas Boxberger
*Department Functionalization Technologies*
*Fraunhofer Institute for Machine Tools and Forming Technology*
Dresden, Germany
0000-0003-4923-3721

Elena Dietrich
*Department Functionalization Technologies*
*Fraunhofer Institute for Machine Tools and Forming Technology*
Dresden, Germany

***Abstract*— In the present work, the load-bearing capacity and stability of a structural component of a robotic arm with adaptive stiffness based on particle jamming were improved. For this purpose, the original concept was combined with the layer jamming approach by designing a biologically inspired scale structure and implementing it in different ways. Various manufacturing processes and designs were examined on the basis of bending tests, with a fabric structure sewn on both sides with TPU scales proving to be the preferred variant. This structure was integrated into a robot segment with a particle jamming core. Further bending tests showed that the integration of layer jamming tripled the holding force.**

***Keywords—adaptive stiffness, layer jamming, particle jamming***

## I. Introduction

Due to their continuum structure, soft robots have a high degree of freedom and can therefore perform complex movements. On the other hand, the soft materials used give them inherent safety, which qualifies them for safe human robot collaboration (HRC). However, in addition to these advantages, they also have a significant disadvantage due to their characteristics: they usually lack stability and holding power, which is a result of their low rigidity [1, 2]. To realize robot structures that are both highly flexible and safe, as well as having an appropriate performance with sufficient load capacity and stability, some approaches with adaptive stiffness have been developed in the past [3, 4]. Various phenomena can serve as triggers for switchability. For example, there are approaches with thermal [3, 5], electrical [6, 7, 8, 9, 10] and magnetic [11, 12] switching triggers. While thermal triggers have the disadvantage that they usually cannot switch very frequently, electrical triggers usually have the problem of safety, as they must work with very high voltages. Magnetic triggers, on the other hand, require very strong magnets close to the point of application, which complicates the system design enormously. One method that works both quickly and safely and enables a simple system design is the jamming effect [5]. In this process, particles or layers are arranged in a flexible, airtight cover in such a way that they can move freely if there is air in the cover. If the cover is evacuated, the particles or layers are pressed together and form a kind of solid body, which increases rigidity. With this approach, switching factors between the stiffened and flexible states of between 100 are possible. However, this approach also has limitations. The filling with particles has the disadvantage that they break off under tensile load and thus reduce the maximum holding force, whereas layers have the disadvantage that they buckle under compressive load. For this reason, initial approaches have been made to combine the two construction methods. By merging particle and layer jamming, it was possible to develop a structure that exhibits good mechanical properties under both tensile and compressive loads. A switching factor of over 300 was achieved. [14]

However, even if this structure shows improved mechanical properties, it is still not suitable for a robot system as it can only be moved in the plane. Motion in all spatial directions is not possible. This paper presents a design that combines the two approaches of particle and layer jamming, based on the biological model of scales, to increase the holding force of a robot structure with adaptive stiffness and to enable movement in all spatial directions.

## II. Concept Development

### A. Biological role model

Layer jamming technology is based on the structural arrangement of layers that achieve increased stiffness through surface contact in their rigid state, while remaining deformable in their flexible state. The design of such systems can be inspired by nature, where scale-like structures often exhibit high multifunctionality and adaptability due to variations in size, morphology and function [6]. The scales of a fish fulfill several functions, including protection against environmental influences and improve swimming efficiency due to their shape and arrangement [6]. The unique combination of high stiffness for stabilization, paired with exceptional flexibility and low weight [7], makes fish scales an ideal bio-inspiration for layer-jamming applications.

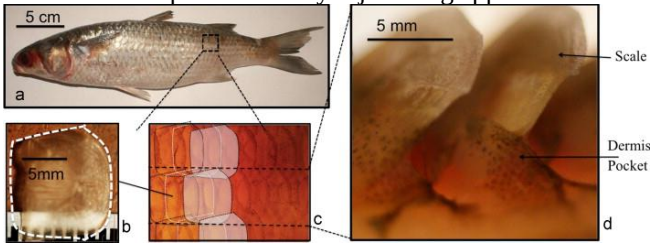


*Figure 1: Arrangement of the scales (c) and their fixation in the dermis (d) [6]*

Fish scales are bone plates that are connected to the dermis, in which they usually sit in small, elastic pockets (Figure 1 (d)). When the skin bends, the pockets open, allowing the plates to move freely to adapt to the shape of the body without bending themselves. In this way, the fish preserves a high degree of flexibility, even though the scales themselves are rigid.

In addition to the friction coefficient of the layers and the contact pressure applied, the contact surface of the layers is crucial for achieving the greatest possible effect of layer jamming. The arrangement of the scales forms a quasi-periodic pattern with alternating, overlapping scales (Figure 1 (c)). This creates contact surfaces that can be used for layer jamming. Different fish species have different forms of scales. In this case, the shape of the cycloid scales was chosen. They have a concentric, circular shape with rounded corners (Figure 1 (b)), which enables optimal sliding on the surrounding scales and reduces the risk of damaging the covering membrane.

### B. *Function demonstrator*

To transfer the biological model into the technical system of a segment for a robot arm, simplified functional demonstrators were first produced in the form of a bending beam (22 mm x103 mm), which should serve to evaluate the developed concepts. The preferred concept was then integrated into a robot segment with a particle jamming core.

Scales are very hard and can damage the sensitive outer cover of the overall system, so they were made softer. Scales measuring 22 mm x 20 mm were cut out of a TPU foil with a thickness of 500 µm and their edges rounded (Figure 2 (a)).

Two concepts were developed for arranging and fixing the film scales in a flexible carrier layer- in concept 1 the base layer is made of silicone and in the second concept it is made of a fabric. For concept 1, 23 scales are cast into a silicone base with a spacing of 2 mm. Therefore, the scales are placed in a mold made of FDM printing (Figure 2 (b)), which is then filled with a 6 mm layer of Silupran 2400 material.

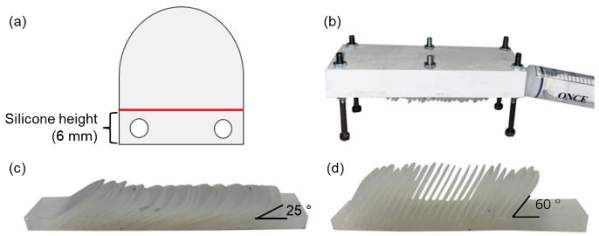


*Figure 2: Concept 1 with silicone layer, scale shape (a), casting procedure (b), flat design (c), steep design (d)*

The orientation of the scales can influence the mechanical behavior of the structure. With a large tilt angle, the scales do not affect each other and can therefore move freely. If the angle of inclination is smaller, the scales are in contact and friction occurs, which can make deformation more difficult. Two different versions of the concept were therefore produced, which differ in the angle of inclination of the scales. In the version with the steeply aligned scales, these are oriented at an angle of 60° (Figure 2 (d)) and for the flat version at 25° (Figure 2 (c)).

For the second concept, 12 scales are sewn 7 mm apart onto a fabric (bi-stretch slinky cyclist jersey) that can be stretched in all directions. Two versions are also produced here, one with scales on one side (Figure 3 (c)) and the other with scales on both sides (Figure 3 (d)).

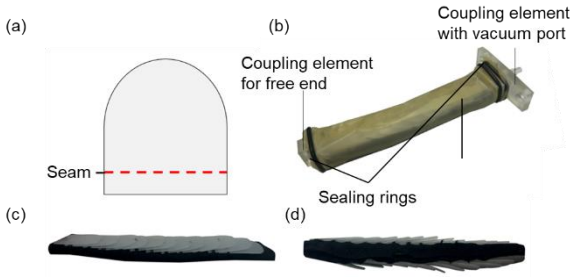


*Figure 3: Concept 2 with fabric layer, scale form (a), one-sided design (c), double-sided design (d), Function demonstrator for bending tests (b)*

The scale structures produced in this way are placed between two 3D-printed coupling elements so that they can be clamped in the testing machine in a defined manner and subjected to a bend. One coupling element is equipped with channels and a connection for the vacuum pump to apply the vacuum. The scale structure is covered by a latex membrane to be able to apply the vacuum required to achieve the jamming effect.

### C. *Bending tests*

To be able to evaluate the developed concepts, tests are carried out on a one-sided clamped bending beam. For this purpose, the functional demonstrators are attached to a vertically aligned mounting plate, which is clamped in an Allround Z020 universal testing machine from ZwickRoell Gmbh & Co. KG, which aligns the demonstrator horizontally. A steel cable with a diameter of 0.5 mm and a length of 600 mm is attached to the free end of the demonstrator, to which a tensile load is applied using the testing machine, resulting in a bending load on the specimen. The long steel cable minimizes the transverse forces generated during bending and enables an almost pure tensile load at the free end of the bending beam.

The tests were carried out at a loading speed of $v = 0.1\ mm/s$ up to a maximum deflection of $u = 30\ mm$. The force-displacement curves of the loading and unloading are recorded to be able to detect reversible deformation components. Three measurements are carried out in the soft and stiff state for each structure, with the structures being returned to their initial horizontal state after each measurement.

For the comparative evaluation, the maximum force in the stiff state $F_{max,stiff}$ before irreversible deformation occurs, the stiffness in both the soft ($k_{soft}$) and stiff state ($k_{stiff}$) and the switching factor K are determined. In the stiff state, a negative differential pressure of 95-97 kPa is applied to trigger the jamming effect. The stiffness is calculated using the formula $k = \Delta F/\Delta u$. In the soft state, the stiffness is evaluated in the range of $u = 10\text{-}20\ mm$, where the behavior is approximately linear. This range is of particular importance as the deformation occurs in the soft state, which makes the mechanical properties particularly interesting for larger deformations. In the stiff state, the stiffness is evaluated in the range of the first linear-elastic increase up to $u = 0.5\ mm$. This range is crucial because it characterizes the mechanical properties in the stiff state before the residual deformation

occurs. The switching factor is calculated using the formula $K = k_{stiff}/k_{soft}$.

The force-displacement curves in Figure 4 show as an example how the application of a vacuum affects the structural behavior.

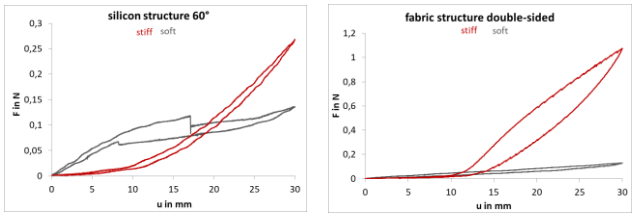


*Figure 4: Force-displacement curves of the steep silicone concept and the double-sided fabric concept*

It can be observed that the silicone structure initially has a steeper rise in the soft state, which flattens out after a deflection of around 5 mm. In the stiff state, the structure initially shows a flat settling behavior, which is probably due to a weak point in the demonstrator structure. A steeper rise is only observed after a deflection of around 10 mm. The fabric structure shows an almost linear behavior in the soft state up to the point of maximum deformation, with a very small increase. In the stiff state, it also shows a settling behavior up to a deflection of about 10 mm, which may also indicate a weak point in the demonstrator. Beyond this range, there is a steep increase followed by a clear hysteresis, which indicates an irreversible element of the deformation.

Due to the settling behavior, the stiffness in the stiff state is determined in the initial range of the increased slope in all tests. The results are listed in Table 1.

*Table 1: Results of the bending test of the functional demonstrators with stiffness in soft ($k_{soft}$) and stiff state ($k_{stiff}$) and switching factor K*

| | $k_{soft}$ | $k_{stiff}$ | $K$ |
|---|---|---|---|
| Silicon 25° | 0,004 N/mm | 0,013 N/mm | 3 |
| Silicon 60° | 0,003 N/mm | 0,010 N/mm | 3 |
| Fabric 1-sided | 0,003 N/mm | 0,012 N/mm | 4 |
| Fabric double-sided | 0,003 N/mm | 0,071 N/mm | 24 |

All concepts show a similarly low stiffness of less than 0.01 N/mm in the soft state. In the stiff state, the double-sided fabric structure shows the highest stiffness of 0.071 N/mm, which leads to a switching factor of 23, while the other structures only have a switching factor of 3.

For this reason, the double-sided textile structure is selected for integration into the robot segment.

## III. System Integration

### A. Integration in robot segment

Based on the bending tests carried out on the functional demonstrators, the preferred concept was determined and integrated into a robot segment of an existing system. This consists of a core made of particles and a cover with layer jamming surrounding the core based on the developed concept of scale structures.

First, two flat scale structures with the dimensions 100 x 120 mm for the inner layer and 100 x 140 mm for the outer layer are produced as described in chapter B. The distance between the individual rows of scales is set at 6 mm, with the arrangement being offset to ensure correct alignment and structural consistency (Figure 5). The resulting flat structures are stitched together to form a two-sided scale structure.

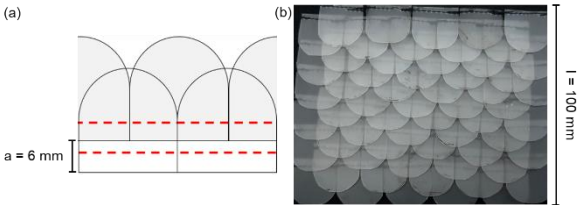


*Figure 5: Flat scale structure for robot segment (a) arrangement, (b) finished structure*

The structure of the overall segment is as follows: The core consists of a silicone tube, which can be used for media guidance, for example. This tube is surrounded by a compression spring located between two coupling elements, holding the channels and the connection for the vacuum application. The core is also enclosed by a tubular chamber filled with particles (specific type not specified), thus realizing the effect of particle jamming. The double-sided layer structure is wrapped around this core, which is then enclosed by a latex membrane to facilitate the application of the vacuum for the layer jamming effect.

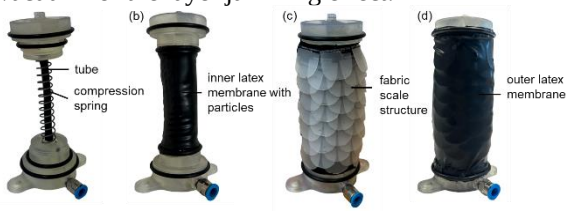


*Figure 6: Structure of the overall segment with particle jamming core and integrated scale structure for layer jamming*

### B. Bending tests

The resulting segment is also characterized in the bending test as described in chapter C and compared with a segment with the same geometric dimensions, which consists only of the particle jamming core.

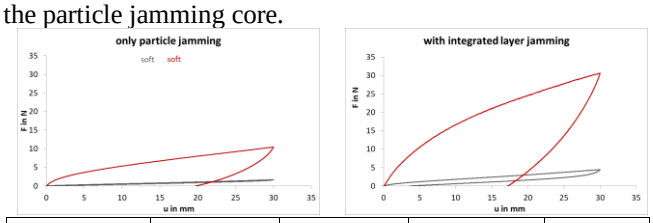


| | $F_{max,stiff}$ | $k_{soft}$ | $k_{stiff}$ | $K$ |
|---|---|---|---|---|
| Particel Jamming | 10,5 N | 0,049 N/mm | 1,054 N/mm | 21,5 |
| Particle + Layer Jamming | 29,9 N | 0,119 N/mm | 2,687 N/mm | 22,6 |

*Figure 7: Force-displacement curves of the concept with particle jamming only (left) and with integrated layer jamming (right) and the determined parameters*

By integrating the layer jamming in the form of a scale structure, the maximum holding force could be almost tripled from approx. 10N to approx. 30N. The stiffness in the rigid state was also more than doubled. The switching factor has remained almost the same, as stiffness in the soft state has also increased.

## IV. References

[1] D. Rus and M. T. Tolley, "Design, fabrication and control of soft robots," *Nature*, 2015.

[2] D. Trivedi, C. D. Rahn, W. M. Kier and I. D. Walker, "Soft robotics: Biological inspiration, state of the art, and future research," *Applied Bionics and Biomechanics,* 2008.

[3] M. Manti, V. Caccuciolo and M. Cianchetti, "Stiffening in Soft Robotics: A Review of the State of the Art," *IEEE RA-M,* p. 93–106, 2016.

[4] L. Wang, Y. Yang, Y. Chen, C. Majidi, F. Iida, E. Askounis and Q. Pei, "Controllable and reversible tuning of material rigidity for robot applications," *Materials Today,* p. 563–576, 2018.

[5] J. R. Capadona, K. Shanmuganathan, D. J. Tyler, S. J. Rowan and C. Weder, "Stimuli-Responsive Polymer Nanocomposites Inspired by the Sea Cucumber Dermis," *Science,* pp. 1370-1374, 2008.

[6] F. Carpi, G. Frediani, C. Gerboni, J. Gemignani and D. De Rossi, "Enabling variable-stiffness hand rehabilitation orthoses with dielectric elastomer transducers," *Medical Engineering and Physics,* 2014.

[7] B. Lui, S. A. Boggs and M. T. Shaw, "Electrorheological properties of anisotropically filled elastomers," *IEEE Transactions on Dielectrics and Electrical Insulation,* pp. 173 - 181, 2001.

[8] C. Cao and X. Zhao, "Tunable stiffness of electrorheological elastomers by designing mesostructures," *Applied Physics Letters,* 2013.

[9] L. Di Lillo, W. Raither, A. Bergamini, M. Zündel and P. Ermanni, "Tuning the mechanical behaviour of structural elements by electric fields," *Applied Physics Letter,* 2013.

[10] T. Wang, J. Zhang, Y. Li, J. Hong and M. Y. Wang, "Electrostatic Layer Jamming Variable Stiffness for Soft Robotics," *IEEE/ASME Transactions on Mechatronics,* pp. 424 - 433.

[11] C. Majidi and R. J. Wood, "Tunable elastic stiffness with microconfined magnetorheological domains at low magnetic field," *Applied Physics Letters,* 2010.

[12] Y. Li, J. Li, T. Tian and W. Li, "A highly adjustable magnetorheological elastomer base isolator for applications of real-time adaptive control," *Smart Materials and Structures,* 2013.

[13] N. Rojas and A. Clark, "Assessing the Performance of Variable Stiffness Continuum Structures of Large Diameter," *IEEE RA-L,* p. 2455–2462, 2019.

[14] W. R. Wockenfuß, L. Weisheit, S. Rieß and W. Kaal, "Structural components with adjustable stiffness for soft robotics," *Konstruktion,* pp. 61-66, 2021.

[15] F. J. Vernerey and F. Barthelat, "Skin and scales o fteleost fish: Simple structure but high performance and multiple functions," *Journal of Mechanics and Physics of Solids,* pp. 66-76, 2014.

[16] P. Rawat, D. Zhu, M. Z. Rahman and F. Barthelat, "Structural and mechanical properties of fish scales for the bio-inspired design of flexible body armors: A review," *Acta Biomaterialia,* pp. 41-67, 2021.